Colloid Polym Sci (2007) 285:1257–1265
DOI 10.1007/s00396-007-1681-1

ORIGINAL CONTRIBUTION

# Drying dissipative patterns of dyes in ethyl alcohol on a cover glass

**Tsuneo Okubo · Naomi Yokota · Akira Tsuchida**

Received: 25 February 2007 / Accepted: 31 March 2007 / Published online: 20 April 2007


**Abstract** Drying dissipative structural patterns formed in the course of drying ethyl alcohol solutions of rhodamine 6G, uranine, 7-hydroxy coumarin, and 7-amino-4-(trifluoro methyl)-coumarin are studied on a cover glass. The macroscopic broad ring patterns form for all the solutions examined, which supported importance of the convectional flow of ethyl alcohol and dye solutes. Dried area increases as dye concentration increases above the critical dye concentration. Microscopic fine patterns including street-like, needle-like, and flower-like crystal structures are formed in the solidification processes. Change in the functional side group moieties of the dyes gives the strong effect on the microscopic drying patterns; even the main chemical structures are same. Kinetic aspect of the drying patterns is studied.

**Keywords** Drying dissipative structure · Pattern formation · Dye · Broad ring pattern · Street-like pattern · Flower-like pattern

T. Okubo
Institute for Colloidal Organization,
Hatoyama 3-1-112, Uji,
Kyoto 611-0012, Japan

T. Okubo (✉)
Cooperative Research Center, Yamagata University,
Johnan 4-3-16,
Yonezawa 992-8510, Japan
e-mail: okubotsu@ybb.ne.jp

N. Yokota · A. Tsuchida
Department of Applied Chemistry, Gifu University,
Yanagido 501-1193, Japan

## Introduction

Generally speaking, most structural patterns in nature form via self-organization accompanied with the dissipation of free energy and in the nonequilibrium state. Among several factors in the free energy dissipation of aqueous colloidal suspensions, evaporation of solvent molecules at the air-solvent interface and the gravitational convection are very important. To understand the mechanisms of the dissipative self-organization of the simple model systems instead of much complex nature itself, the authors have studied the *convectional*, *sedimentation*, and *drying* dissipative patterns of suspensions and solutions as systematically as possible.

*Drying* dissipative patterns have been studied for suspensions and solutions of many kinds of colloidal particles [1–15], linear-type polyelectrolytes [16], water-soluble nonionic polymers [17, 18], biopolymers [19], ionic and nonionic detergents [9, 20, 21], and gels [22] mainly on a cover glass. The macroscopic broad ring patterns of the hill, accumulated with spheres in the outside edges, always formed. For the nonspherical particles, the round hill was formed in the central area in addition to the broad ring. Macroscopic spoke-like cracks or fine hills including flickering spoke-like ones were also observed for many solutes. The convection of water and the solute molecules at different rates under gravity and the translational and rotational Brownian movement of the latter were important for the macroscopic pattern formation. Furthermore, beautiful fractal patterns, such as branch-like, arc-like, block-like, star-like, cross-like, and string-like ones, were observed in the microscopic scale. These microscopic drying patterns were reflected from the *shape*, *size*, and *flexibility* of the solute molecules themselves. In other words, our experiments on the drying dissipative structures support an idea that information of solutes, such as their *size*, *length*, *shape*,

**Scheme 1** Chemical structure of dyes

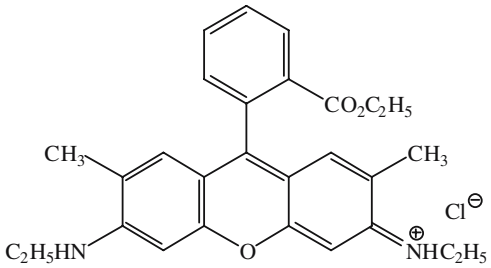


Rhodamine 6G

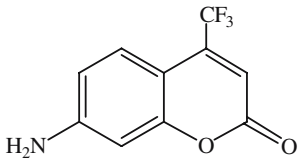


7-Amino-4-(trifluoromethyl)coumarin

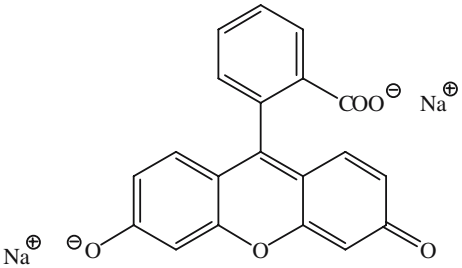


Uranine

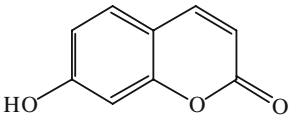


7-Hydroxycoumarin

*width*, and *rigidity*, for example, are transformed into the drying patterns. It is highly plausible that the information transfer takes place quite efficiently in the process of solidification from solution or suspension at high concentration. At high concentration condition, the striking stereospecific packing effect among solutes and further orientation effect of the neighboring solutes intermediated by the ionic, hydrophobic, hydrogen-bonding, and polar moieties of solutes, for example, must play an important role for the drying pattern formation. Microscopic patterns also supported importance of the electrostatic and the hydrophobic interactions between solutes and/or between the solutes and substrate in the course of solidification. One of the important findings in our experiments was that the primitive vague patterns were formed already in the suspension state before dryness, and they grew toward fine structures in the course of solidification.

Recently, the *sedimentation* dissipative patterns have been studied in the course of drying suspensions of colloidal silica spheres and green tea in a glass dish, a watch glass, and others [23–26]. The broad ring patterns also formed within 30 min in suspension state at room temperature by the convectional flow of water and the colloidal particles. The important finding here was that the sedimentary particles were suspended above the substrate and always moved by the external fields including convectional flow and the sedimentation of the particles by the gravity.

The *convectional* dissipative structures were studied for the Chinese black ink and the 100% ethanol suspensions of colloidal silica spheres in our laboratory [10, 27]. The existence of the small circle-like *convection cells*, proposed by Terada et al. [28–30], for the first time, was supported. Vigorous convectional cell-like flow was observed for the suspensions with the naked eyes, and the patterns changed dynamically with time.

In this work, drying dissipative patterns of dye molecules in ethyl alcohol have been studied on a cover glass in the macroscopic and microscopic scales. Frankly speaking,

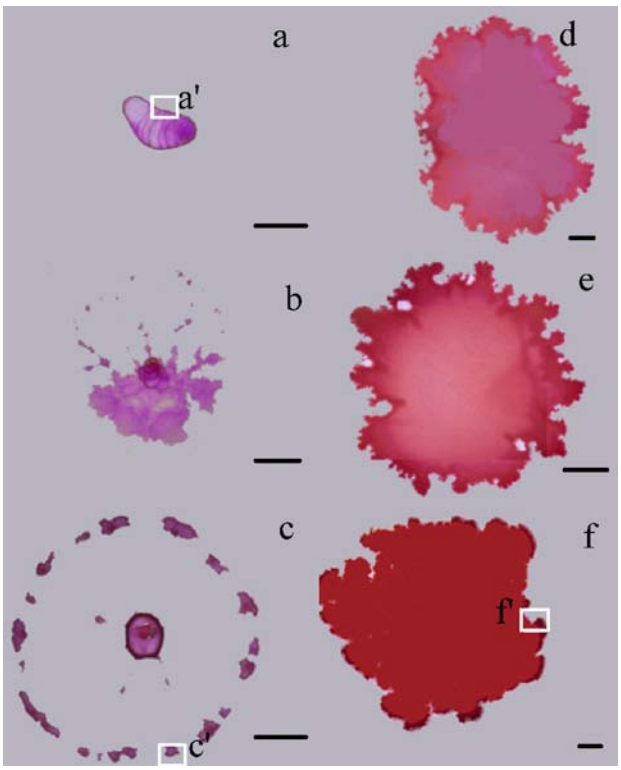


**Fig. 1** Drying dissipative patterns of rhodamine 6G in ethanol on a cover glass at 25 °C. **a** 0.0001 M, **b** 0.0005 M, **c** 0.001 M, **d** 0.005 M, **e** 0.01 M, **f** 0.1 M, $V$=10 μl, length of the bar is 2.0 mm

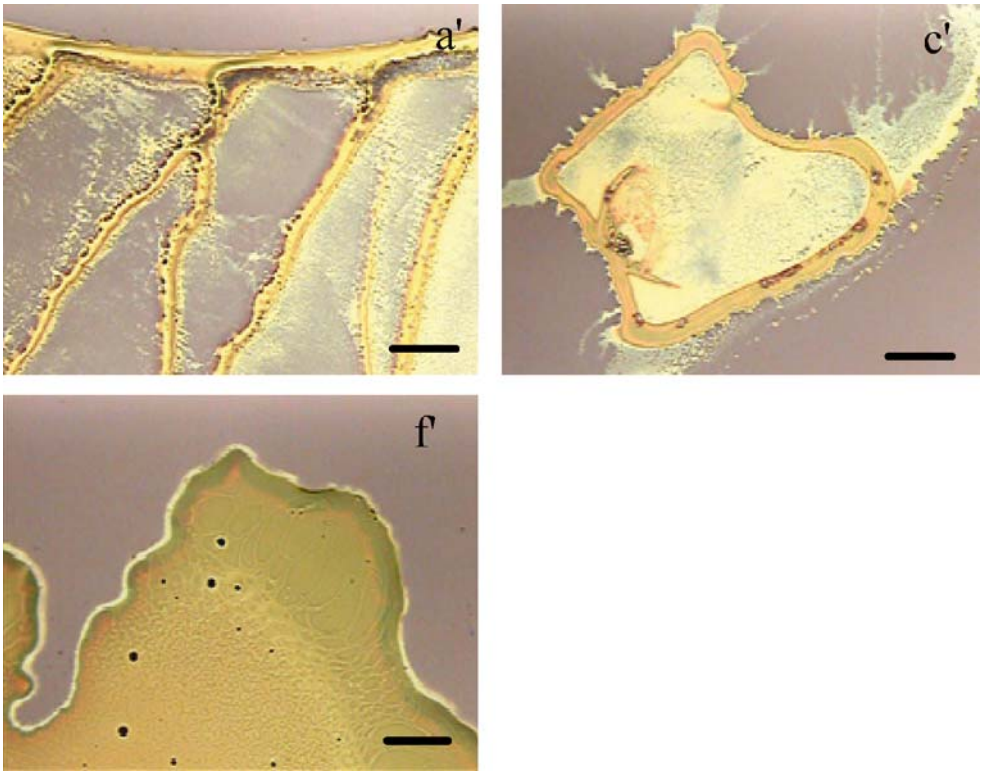


**Fig. 2** Drying dissipative patterns of rhodamine 6G in ethanol on a cover glass at 25 °C. **a′** 0.0001 M, **c′** 0.001 M, **f′** 0.1 M, $V$=10 ml, length of the bar: 100 μm (**a′**, **c′**), 200 μm (**f′**)

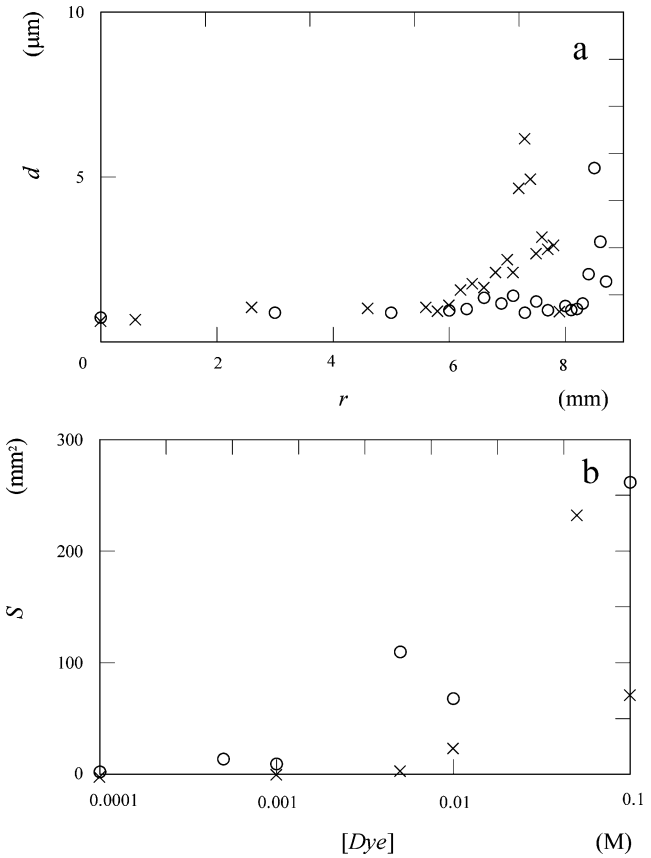


**Fig. 3** Thickness of the drying film ($d$, **a**) as a function of the distance from the center ($r$) and drying area ($S$, **b**) as a function of dye concentration for rhodamine 6G (open circle) and uranine (*times symbol*) in ethanol on a cover glass at 25 °C. $V$=10 μl, **a** [rhodamine 6G]=0.1 M, [uranine]=0.1 M

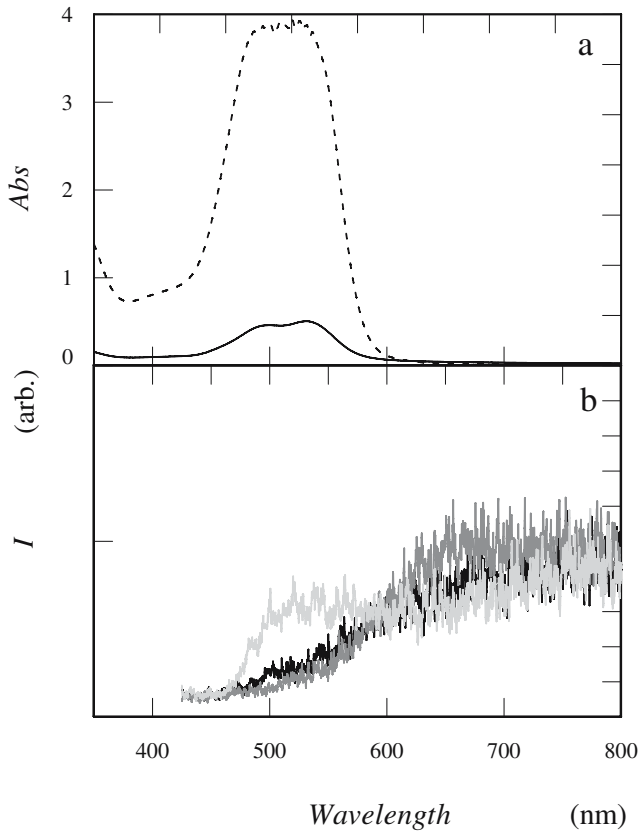


**Fig. 4** Absorption and fluorescence spectra of rhodamine 6G on a cover glass at 25 °C. *Solid curve* 0.01 M, *dotted curve* 0.1 M, *broken curve* cover glass only

two books written by Nakaya [31] and Boys [32] introduced the drying experiments of dyes reported in this paper to the authors.

## Experimental

### Materials

Rhodamine 6G, uranine, 7-hydroxy coumarin, and 7-amino-4-(trifluoro methyl)-coumarin were purchased from Wako Pure Chemicals (Tokyo) and used without further purification. Molecular structures of these dyes are shown in Scheme 1. Ethyl alcohol (spectrum grade) was purchased from Wako. Water used for rinsing the glasswares was purified by a Milli-Q reagent grade system (Milli-RO5 plus and Milli-Q plus, Millipore, Bedford, MA).

### Observation of the dissipative structures

The Ethanol solutions of the dyes (10 or 5 μl) were dropped carefully and gently onto a micro-cover glass (30 mm× 30 mm, thickness no. 1, 0.12 to 0.17 mm, Matsunami Glass, Kishiwada, Osaka) set in a glass dish (60 mm in diameter, 15 mm in depth, Petri, Tokyo). The cover glasses were used without further rinse. The contact angle of the pure water with a cover glass was 31±0.5° from the drop profiles of water on the unrinsed cover glass, respectively. Extrapolation to the zero amount of water was made from the measurements at the several amounts of water. A micropipet (Multi-pet Plus, Eppendorf, UK) was used for the dropping.

Observation of the drying patterns was made for the film formed after the solutions were dried up completely on a cover glass in a room air-conditioned at 25 °C and 45 to

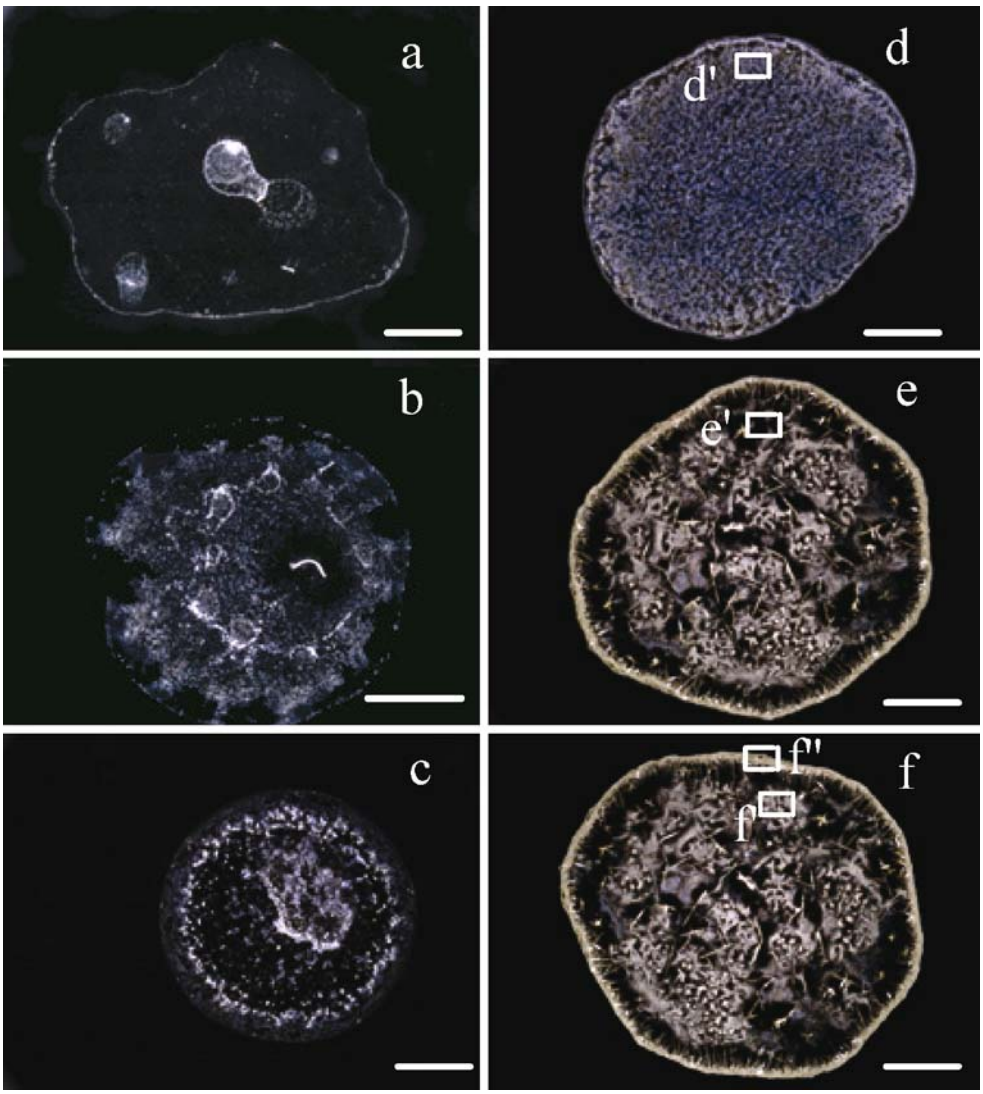


**Fig. 5** Drying dissipative patterns of 7-amino-4-(trifluoro methyl)-coumarin in ethanol on a cover glass at 25 °C. (**a**) 0.00005 M, (**b**) 0.0001 M, (**c**) 0.0004 M, (**d**) 0.001 M, (**e**) 0.004 M, (**f**) 0.04 M, $V$=10 μL, length of the bar is 2.0 mm

60% in humidity. The humidity was not regulated in our experiments. Microscopic dissipative structures were observed with a laser 3D profile microscope (type VK-8500, Keyence), a digital high definition (HD) microscope (type VH-7000 Keyence, Osaka), and videotape recorder (WV-ST1, Sony). Microscopic structures were also observed with a metallurgical microscope (PME-3, Olympus, Tokyo). Macroscopic close-up pictures were also taken on a Canon EOS 55 camera with a macro-lens (EF50mm, $f$= 2.5) and a life-size converter EF.

Absorption and fluorescence spectra were taken on a Hitachi Spectrophotometer (type U-3500, Tokyo) and a Hitachi Fluorescence Spectrophotometer (type F-4500).

## Results and discussion

### Drying dissipative patterns of rhodamine 6G and uranine

Figure 1 shows the drying patterns of rhodamine 6G, one of the cationic dyes, on a cover glass, where the solute concentrations range from 0.0001 M (a) to 0.1 M (f). Amount of liquid ($V$) was 10 μl. The size of the dropped liquid on a cover glass was wide, about 20 mm in diameter irrespective of dye concentrations. The main reason for the wide spreading of the liquids is ascribed to the low surface tension of ethyl alcohol (22 dyn/cm at 20 °C) compared with that of water (73 dyn/cm at 20 °C). The dried area ($S$, see also Fig. 3b) shrank significantly when the dye concentrations were below 0.001 M, which suggests that the contact angle of the dye solution was high especially at the low dye concentrations and the liquid frontier moved toward center accompanied with the dye solutes. At 0.001 M, the dried areas separated into the central area and the ring at the initial outside frontier region of the liquid as is shown in Fig. 1**c**. Above 0.005 M, on the other hand, the dried area increased as the dye concentration increased, which supports the interfacial tensions of the liquids with a cover glass being low enough to prevent shrinking of the liquid in the course of drying. Clearly, broad ring patterns were always observed for all the solutions examined.

A main cause for the broad ring formation is due to the convection flow of ethyl alcohol solvents and dye solutes in the different rates, where the rate of the latter will be slower than that of the former under gravity. Especially, flow of the dyes from the center area toward the outside edges in the lower layer of the liquid, which was observed on a digital HD microscope directly from the movement of the very rarely occurred aggregates of the colloidal particles of Chinese black ink, is important [10]. Clearly, the convectional flow is enhanced by the evaporation of ethyl alcohol at the liquid surface, resulting to the lowering of the solution temperature in the upper region of the solution. When the dyes reach the edge wall on a cover glass at the outside region of the liquid, a part of the dye solutes will turn to upward and go back to the center region. However, many large dyes may drop downward on the cell bottom close to the outside cell wall, where the effective horizontal flow of the dyes may stop temporarily with help of the

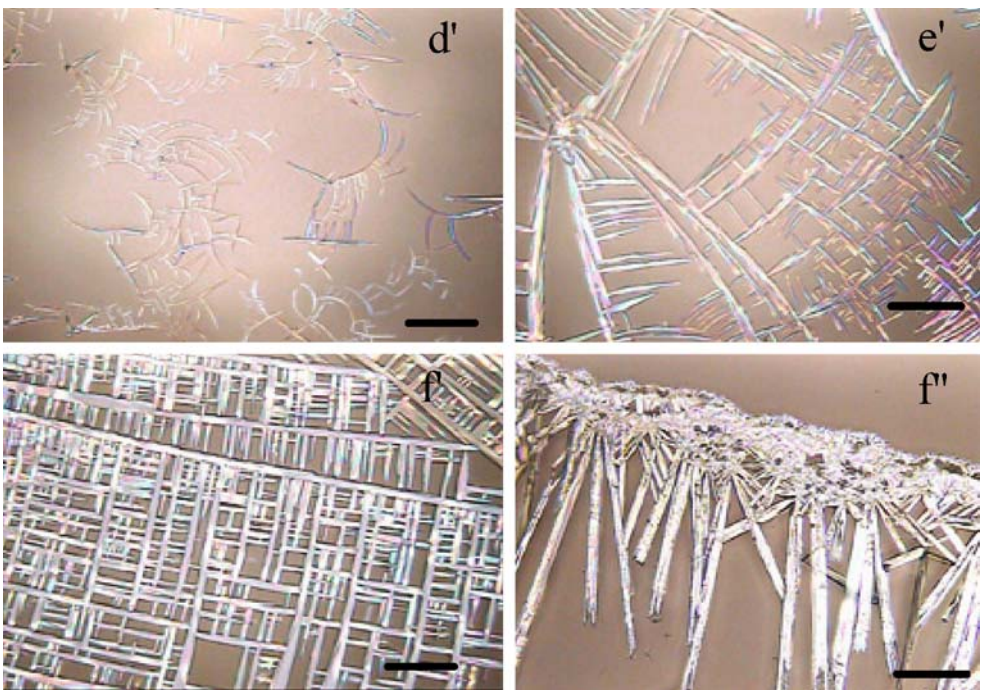


**Fig. 6** Drying dissipative patterns of 7-amino-4-(trifluoro methyl)-coumarin in ethanol on a cover glass at 25 °C. **d′** 0.001 M, **e′** 0.004 M, **f′**, **f″**) 0.04 M, $V$=10 μL, length of the bar: 20 μm (**d′**, **e′**, **f′**), 100 μm (**f″**)

affinitive interactions between dyes and the glass cell wall. This process is further followed by the broad ring accumulation of the dyes near the round outside edges.

The broad ring formation in the dried film has been observed so often for most of the solutions and suspensions examined by our group [7–14, 16–25] and by other researchers [1–6]. Recently, microgravity experiments were made for the observation of the drying dissipative patterns of deionized suspension of colloidal silica spheres [33]. Surprisingly, the broad ring patterns did not disappear even in microgravity. This supports strongly that both the gravitational and the Marangoni convections contribute to

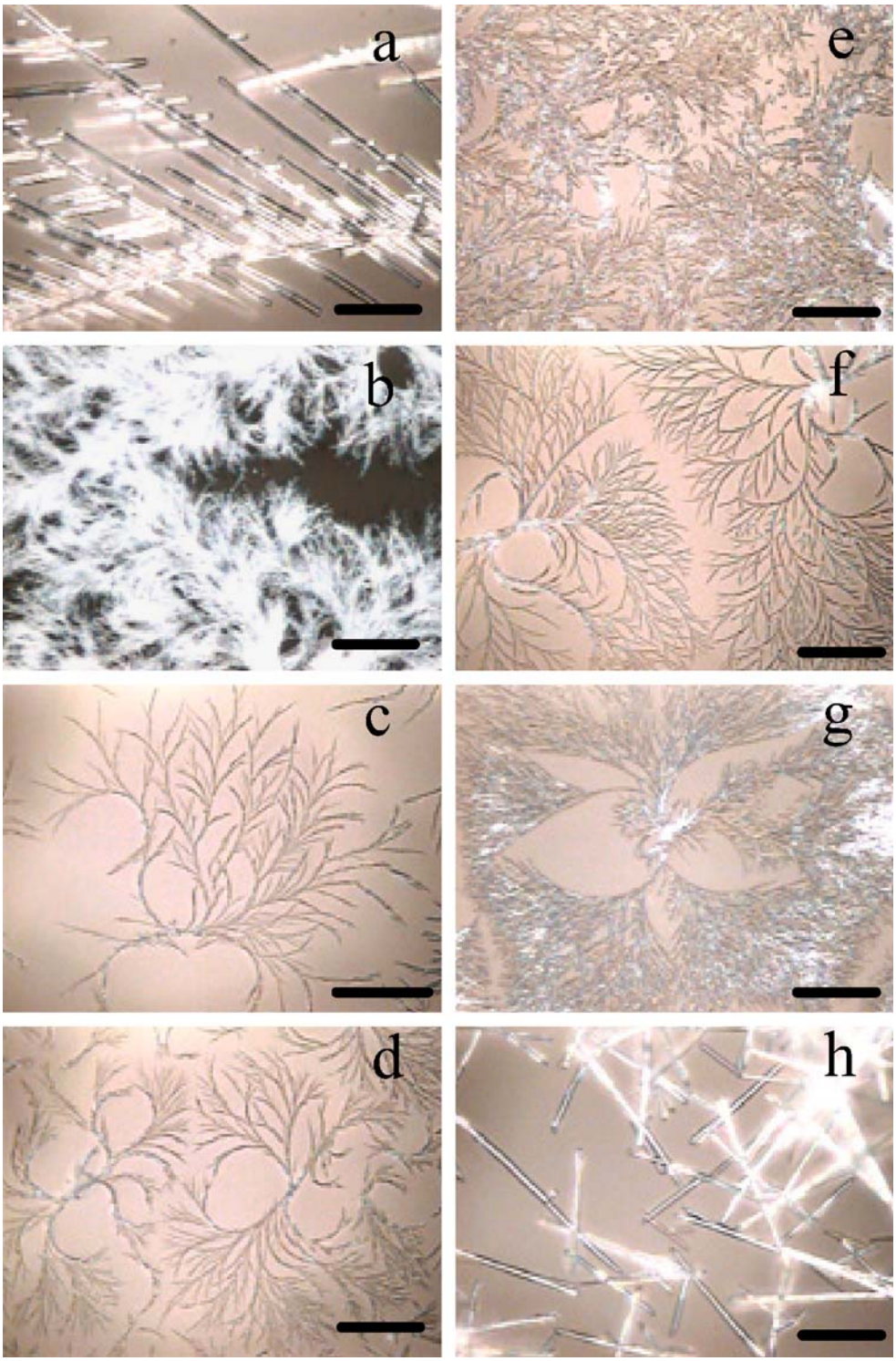


**Fig. 7** Drying dissipative patterns of 7-hydroxy coumarin in ethanol on a cover glass at 25 °C. **a** 0.001 M, **b** 0.0015 M, **c** 0.002 M, **d** 0.005 M, **e** 0.01 M, **f** 0.025 M, **g** 0.05 M, **h** 0.1 M, $V$=10 μl, length of the bar is 20 μm

the broad ring formation on earth, and the latter is still important in microgravity. We should note further here that the broad ring patterns, which were generally observed for all drying patterns of suspensions and solutions on a cover glass including the present paper, were formed already in the process of convectional flow of water and solutes in suspension state. The broad rings in the sedimentation structures have been observed for the colloidal suspensions in a polystyrene dish [21], a glass dish [21], a watch glass [22], and even a deep bowl [23].

It should be mentioned here that shape of the outer edges of the dried films of rhodamine 6G and uranine were not smooth and round, but bumpy (see Fig. 1 for rhodamine 6G). The similar bumpy patterns have been observed only once in our laboratory for aqueous dispersions of colloidal silica spheres (103 nm in diameter) in the presence of sodium chloride on a cover glass [7]. The reason for this observation is, however, not clear yet.

Figure 2 shows the extended microscopic pictures of the square areas shown in Fig. 1. The broad rings are seen in the outside edges. Furthermore, the spoke-like hills perpendicular to the broad rings were observed close to the broad rings (see Fig. 2a′ and f′). The inner areas were covered with the block-like patterns (see Fig. 2f′), part of which distributed regularly. The macro- and microstructures of the uranine were very similar to those of rhodamine 6G, and the pictures showing these are omitted in this article.

Figure 3a shows the thickness of the dried film of rhodamine 6G and uranine as a function of the distance from the center of the film. Formation of the single broad rings is clear for the cationic and anionic charged dyes. Figure 3b shows the area of the dried film as a function of the dyes. Substantial increase in the dried area is clear when the dye concentration is higher than approximately 0.001 M, which is ascribed to the decrease in the interfacial tensions between the dye solutions and a cell glass.

Figure 4a and b shows the absorption and the fluorescence spectra of the dried film of rhodamine 6G at 0.01 M (solid curve) and 0.1 M (dotted curve). Strong absorption was observed, and the peak wavelengths estimated from the double peak profiles were around 490 and 520 nm. These values were very close to the corresponding peak wavelengths of the methyl alcohol solutions of rhodamine 6G (0.1 M), approximately 485 and 527 nm, respectively, which were observed by the authors. This agreement supports strongly that the former and the latter peaks are ascribed to the absorptions from the monomers and aggregates of rhodamine 6G, respectively. Fluorescent intensities of the dried films were quite low compared with those of ethyl alcohol solution and almost neglected within experimental errors as is seen in Fig. 4b, where the broken curve shows the fluorescence spectrum of cover glass substrate itself. It is highly plausible that the energy migration and quenching of the fluorescent light took place substantially for the film.

The drying patterns of uranine were quite similar to those of rhodamine 6G, although the graphs showing this were omitted in this paper to save space. Striking, shrinking of the dried area took place below 0.01 M. The coexistence of the broken ring and the shrinking occurred when the dye concentrations were 0.001, 0.005, and 0.01 M. At the dye concentrations of 0.05 and 0.1 M, no shrinking took place, and the clear broad rings were observed at the outside edges of the films. It should be noted that formation of the broad

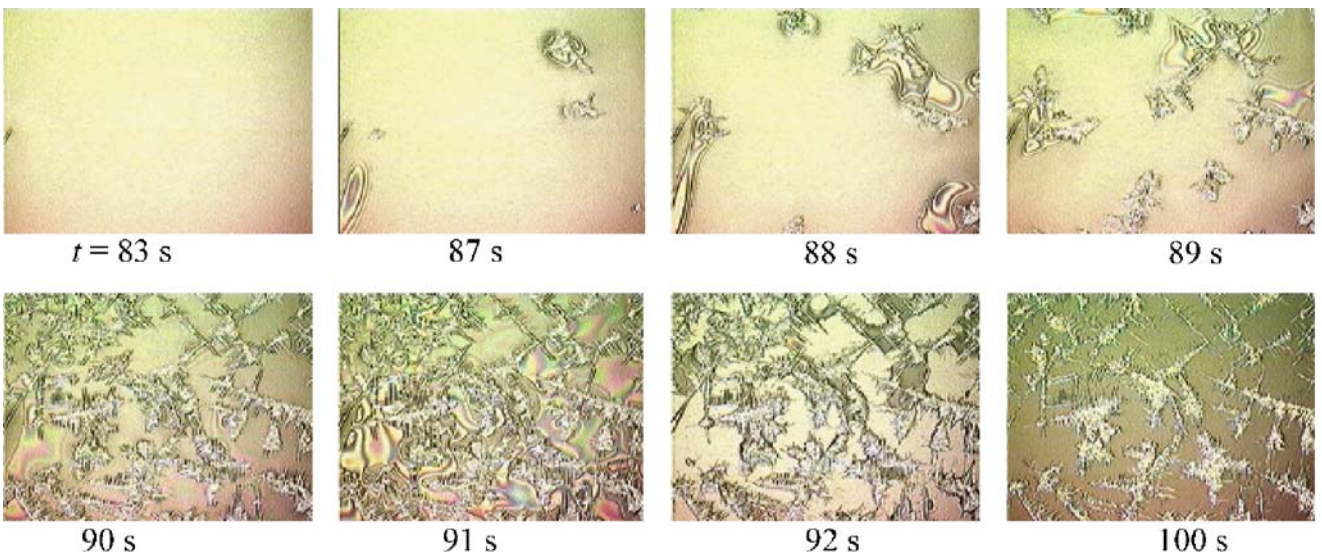


**Fig. 8** Dissipative patterns in the course of drying ethanol solution of 7-amino-4-(trifluoro methyl)-coumarin on a cover glass at 25 °C. $V$=5 μL, 0.04 M, length of the bar is 30 μm

ring is also clear from Fig. 3a. Figure 3b also demonstrates that the $S$ values increased significantly when the dye concentrations increased above 0.001 M.

Drying dissipative patterns of ethyl alcohol solutions of 7-amino-4-trifluoromethy coumarin and 7-hydroxy coumarin

Figure 5 shows the drying patterns of 7-amino-4-fluoromethyl coumarin, one of the weakly acidic dyes, on a cover glass. From Fig. 5a to f, concentrations range from $4\times10^{-5}$ to 0.04 M in ethyl alcohol. At $4\times10^{-5}$ and $1\times10^{-4}$ M, shrinking of the dye area took place slightly with coexistence of the broad ring at the location of the outside edges of the initial liquids. All the pictures in Fig. 5 show that many dye molecules distribute inside the broad ring. This suggests that the 7-amino-4-trifluoromethyl coumarin dyes apt to associate (or stack) in solution state and convectional movement of the dye solutes is difficult compared with that of the spherical and nonassociated solutes. Accumulation of the aggregated and nonspherical colloidal solutes in the center area has been observed clearly in the drying patterns of fractionated bentonites [12].

The extended pictures of the drying patterns are shown in Fig. 6. The beautiful street-like crystallized patterns formed. These microscopic crystal structures were formed clearly in the process of solidification. It should be noted that the crystallized patterns are consistent with the stack association of the dye molecules in solution state. It should be mentioned here that the fluorescence intensity from the dried film of 7-amino-4-trifluoromethyl coumarin was large when excitation wavelength was 380 nm, although the graph showing this was omitted in this paper. The drying patterns of 7-hydroxy coumarin, one of the nonionic dyes on a cover glass were similar to those of 7-amino-4-trifluoro coumarin, although the shrinking of the dry area took place much clearly at 0.001 and 0.0015 M compared with those of latter dyes.

Figure 7 shows the extended microstructures of 7-hydroxy coumarin. Flower-like curved crystals are impressive to observe at the initial dye concentrations from 0.0015 to 0.05 M. It is interesting to note that the needle-like patterns appeared both at the low (0.001 M) and high concentrations (0.1 M) of 7-hydroxy coumarin. Furthermore, it is surprising to note that slight change in the location of the polar and nonpolar group moieties gives the substantial influence on the crystal structures even the main chemical structures are the same between 7-amino-4-trifluoromethyl coumarin and 7-hydroxy coumarin.

When ethyl alcohol solution of 7-amino-4-trifluoromethyl coumarin was dried on a cover glass at 25 °C, drying process started from the outside drying frontiers toward inside. Within 50 s, the broad ring formed at the outside edges, and the crystallized patterns further started to form in the inner area of the broad ring after about 80 s. Figure 8 shows the typical example of the time-resolved microscopic pictures at the certain place in the inner area. At $t$=83 s, all the area observed was solution state, and crystallization started 87 s after setting. However, between time between 87 and 88 s, the small crystal islands moved suddenly and spontaneously in the solution sea. After 88 s, the islands kept their positions and continued to grow. As is clear in the pictures, the nucleation and the crystallization processes took place simultaneously especially in the beginning stage of drying from 88 to 91 s. The aging processes looked to start after 91 s. At $t$=100 s, the drying process was almost completed at the room temperature 25 °C.

**Acknowledgments** Financial supports from the Ministry of Education, Culture, Sports, Science and Technology, Japan and Japan Society for the Promotion of Science are greatly acknowledged for Grants-in-Aid for Scientific Research of Germ Area (17655046) and Scientific Research (B) (16350124 and 18350057), respectively.

## References

1. Vanderhoff JW (1973) J Polym Sci Polym Symp 41:155
2. Nicolis G, Prigogine I (1977) Self-organization in non-equilibrium systems. Wiley, New York
3. Ohara PC, Heath JR, Gelbart WM (1997) Angew Chem 109:1120
4. Maenosono S, Dushkin CD, Saita S, Yamaguchi Y (1999) Langmuir 15:957
5. Nikoobakht B, Wang ZL, El-Sayed MA (2000) J Phys Chem 104:8635
6. Ung T, Litz-Marzan LM, Mulvaney P (2001) J Phys Chem B 105:3441
7. Okubo T, Okuda S, Kimura H (2002) Colloid Polym Sci 280:454
8. Okubo T, Kimura K, Kimura H (2002) Colloid Polym Sci 280:1001
9. Okubo T, Kanayama S, Kimura K (2004) Colloid Polym Sci 282:486
10. Okubo T, Kimura H, Kimura T, Hayakawa F, Shibata T, Kimura K (2005) Colloid Polym Sci 283:1
11. Okubo T, Yamada T, Kimura K, Tsuchida A (2005) Colloid Polym Sci 283:1007
12. Yamaguchi T, Kimura K, Tsuchida A, Okubo T, Matsumoto M (2005) Colloid Polym Sci 283:1123
13. Okubo T, Nozawa M, Tsuchida A (2006) Colloid Polym Sci (in press). DOI 10.1007/s00396-006-1626-0
14. Okubo T, Kimura K, Tsuchida A (2007) Colloids Surfaces B 56:201
15. Okubo T, Nakayama N, Tsuchida A (2007) Colloid Polym Sci, submitted
16. Okubo T, Kanayama S, Ogawa H, Hibino M, Kimura K (2004) Colloid Polym Sci 282:230
17. Shimomura M, Sawadaishi T (2001) Curr Opin Colloid Interface Sci 6:11
18. Okubo T, Yamada T, Kimura K, Tsuchida A (2006) Colloid Polym Sci 284:396
19. Okubo T, Onoshima D, Tsuchida A (2007) Colloid Polymer Sci (in press). DOI 10.1007/s00396-007-1645-5
20. Kimura K, Kanayama S, Tsuchida A, Okubo T (2005) Colloid Polym Sci 283:898

21. Okubo T, Shinoda C, Kimura K, Tsuchida A (2005) Langmuir 21:9889
22. Okubo T, Itoh E, Tsuchida A, Kokufuta E (2006) Colloid Polym Sci 285:339
23. Okubo T (2006) Colloid Polym Sci 284:1395
24. Okubo T (2006) Colloid Polym Sci 284:1191
25. Okubo T (2006) Colloid Polym Sci 285:331
26. Okubo T, Okamoto J, Tsuchida A (2007) Colloid Polymer Sci (in press, 305 nm)
27. Okubo T (2006) Colloid Polym Sci 285:225
28. Terada T, Yamamoto R, Watanabe T (1934) Proc Imp Acad Tokyo 10:10
29. Terada T, Yamamoto R, Watanabe T (1934) Sci Pap Inst Phys Chem Res Jpn 27:75
30. Terada T, Yamamoto R (1935) Proc Imp Acad Tokyo 11:214
31. Nakaya U (1947) Memoirs of Terada Torahiko (Japanese). Kohbunsya Books, Japan
32. Boys CV (1959) Soap Bubbles, Japanese Ed (Yada Y). Maki Books
33. Tsuchida A, Okubo T (2003) Sen'i Gakkaishi 59:264